7964 *Inorg. Chem.* **2010**, *49*, 7964–7968
DOI: 10.1021/ic101001e

Inorganic Chemistry
Article

Structure and Dynamics of the Chromate Ion in Aqueous Solution. An ab Initio QMCF-MD Simulation

Ernst Hinteregger, Andreas B. Pribil, Thomas S. Hofer, Bernhard R. Randolf, Alexander K. H. Weiss, and Bernd M. Rode*

Theoretical Chemistry Division Institute of General, Inorganic and Theoretical Chemistry, University of Innsbruck, Innrain 52a, A-6020 Innsbruck, Austria

Received May 19, 2010

An ab initio quantum-mechanical charge-field molecular-dynamics (QMCF-MD) simulation of the chromate ion in aqueous solution at ambient temperature was performed to study the structure and dynamics of this ion and its hydration shell. In contrast to conventional quantum-mechanical molecular-mechanics molecular-dynamics (QM/MM-MD) simulations, the QMCF-MD approach offers the possibility of investigating composite systems with the accuracy of a QM/MM method but without the time-consuming construction of solute−solvent potential functions. The data of the simulation give a clear picture of the first hydration shell of the chromate anion, which consists of 14 water molecules. The mean distance between the oxygen atoms of the chromate and the hydrogen atoms of water is 1.82 Å. Each chromate oxygen atom is in average coordinated to 2.6 water molecules. The first-shell mean ligand residence time was evalulated as 2.2 ps; the vibrational frequency of the ν_{OH} mode was found to be 185 cm^{-1}. Several structural parameters such as the radial distribution functions, angular distribution functions, and coordination number distributions enable a full characterization of the embedding of the chromate ion in the solvent water. The dynamics of the hydration structure are described by mean residence times of the water molecules in the first hydration shell, distance plots, and velocity autocorrelation functions.

1. Introduction

Chromates are salts of chromic acid (H_2CrO_4) and contain the tetrahedral chromate anion CrO_4^{2-}. The oxidation state of the chromium atom is VI+, corrsponding to a d^0 state. In aqueous solution, chromate and dichromate exist in a chemical equilibrium, which depends on the pH value and is shown in eqs 1−4.

$$CrO_4^{2-} + H_3O^+ \rightleftharpoons HCrO_4^- + H_2O \quad (1)$$

$$HCrO_4^- + H_3O^+ \rightleftharpoons H_2CrO_4 + H_2O \quad (2)$$

$$2HCrO_4^- \rightleftharpoons Cr_2O_7^{2-} + H_2O \quad (3)$$

$$2CrO_4^{2-} + 2H_3O^+ \rightleftharpoons Cr_2O_7^{2-} + 3H_2O \quad (4)$$

Already in weak alkaline solutions the chromate ion is the main species. The equilibrium constants for different pH values have been determined by photometric measurements and electrochemistry.[1−5]

There are some rare chromate minerals. The most common natural occurrence is Krokoit ($PbCrO_4$).

Chromates are very toxic and carcinogenic, and especially the highly water-soluble chromate compounds of the first and second group metals are hazardous for the groundwater.[6] It is important, therefore, to understand the behavior of chromate in aqueous solution. Some experimental data for the structure of chromate in solution have been reported by Hoffmann et al.[7] Simulations of CrO_4^{2-} in water have not been previously published, to our best knowledge, because it is very difficult to construct the potentials for a classical or conventional quantum-mechanical molecular-mechanics molecular-dynamics (QM/MM-MD) simulation.

2. Methods

The ab initio quantum-mechanical charge-field molecular dynamics (QMCF-MD) is an advancement of the intensely used conventional QM/MM methodology (e.g., see refs 8−11). The QMCF methodology enables the straightforward

*To whom correspondence should be addressed. E-mail: Bernd.M.Rode@uibk.ac.at. Tel: +43-512-507-5160. Fax: +43-512-507-2714.

(1) Holleman, A. F.; Wiberg, E.; Wiberg, N. *Lehrbuch der Anorganischen Chemie*; de Gruyter: Berlin, 1995; Vol. *101*, pp 1443−1446.
(2) Linge, H. G.; Jones, a. L. *Aust. J. Chem.* **1968**, *21*, 1445.
(3) Linge, H. G.; Jones, a. L. *Aust. J. Chem.* **1968**, *21*, 2189.
(4) Haight, G. P., Jr.; Richardson, D. C.; Coburn, N. H. *Inorg. Chem.* **1964**, *3*, 1777–1780.
(5) Sasaki, Y. *Acta Chem. Scand.* **1962**, *16*, 719–734.
(6) Costa, M.; Klein, C. B. *Crit. Rev. Toxicol.* **2006**, *36*, 155–163.
(7) Hoffmann, M. M.; Darab, J. G.; Fulton, J. L. *J. Phys. Chem.* **2001**, *105*, 1772–1782.
(8) Tongraar, A.; Rode, B. M. *Phys. Chem. Chem. Phys.* **2003**, *5*, 357.
(9) Rode, B. M.; Hofer, T. S. *Pure Appl. Chem.* **2006**, *78*(25), 525–539.
(10) Hofer, T. S.; Tran, H. T.; Schwenk, C. F.; Rode, B. M. *J. Comput. Chem.* **2004**, *25*, 211–221.
(11) Hofer, T. S.; Pribil, A. B.; Randolf, B. M.; Rode, B. M. *J. Am. Chem. Soc.* **2005**, *127*, 14231–14238.

 Published on Web 08/12/2010

simulation of strongly polarizing ions like U^{4+}[12] and of systems with low symmetry,[13] for which solute−solvent potentials are very difficult to obtain. To avoid this problem, the QM region in the QMCF methodology is enlarged and divided into two parts. Hence, the simulation box has three regions with different calculation levels: the QM zones (core and layer) and the MM region. Ab initio calculations are applied in the inner QM region, called the core, where the solute is situated, mostly hydrated with some solvent molecules, and in the extended QM zone, the layer part, which consists exclusively of solvent molecules. This arrangement allows one to neglect the non-Coulomb forces between the core zone and the outer MM region. The forces in the different zones are calculated according to eqs 5−7:

$$F_J^{\text{core}} = F_J^{\text{QM}} + \sum_{I=1}^{M} \frac{q_I^{\text{MM}} q_J^{\text{QM}}}{{r_{IJ}}^2} \left[1 + 2\frac{\varepsilon+1}{2\varepsilon-1}\left(\frac{r_{IJ}}{r_c}\right)^3\right] \quad (5)$$

$$F_J^{\text{layer}} = F_J^{\text{QM}} + \sum_{I=1}^{M} \frac{q_I^{\text{MM}} q_J^{\text{QM}}}{{r_{IJ}}^2} \left[1 + 2\frac{\varepsilon+1}{2\varepsilon-1}\left(\frac{r_{IJ}}{r_c}\right)^3\right] + F_{IJ}^{\text{nC}} \quad (6)$$

$$F_J^{\text{MM}} = \sum_{\substack{I=1 \\ I\neq J}}^{M} F_{IJ}^{\text{MM}} + \sum_{I=1}^{N_1+N_2} \frac{q_I^{\text{MM}} q_J^{\text{QM}}}{{r_{IJ}}^2} \left[1 + 2\frac{\varepsilon+1}{2\varepsilon-1}\left(\frac{r_{IJ}}{r_c}\right)^3\right] + \sum_{I=1}^{N_2} F_{IJ}^{\text{nC}} \quad (7)$$

F^{core} corresponds to the forces acting on particle J in the core zone derived by quantum mechanics, F_J^{layer} to the forces acting on particle J located in the layer, and F_J^{MM} to the forces acting on particle J in the MM region. The sum over F_{IJ}^{nC} represents the non-Coulomb contributions between water in the layer zone and bulk. To ensure a smooth transition between the QM and MM parts of the simulation, a smoothing function is applied, which guarantees a continuous transition of particles between the layer and MM regions. This smoothing region has a standard thickness of 0.2 Å and is realized by eq 8:

$$F_J^{\text{smooth}} = S(r)\,(F_J^{\text{layer}} - F_J^{\text{MM}}) + F_J^{\text{MM}} \quad (8)$$

$S(r)$ denotes the smoothing function, where r is the distance of a given solvent molecule from the center of the core zone, r_0 is the radius of the whole ab initio calculated region, and r_1 is the inner border of the smoothing region.

$$S(r) = \begin{cases} 1 & \forall\ r \le r \\ \dfrac{({r_0}^2 - r^2)^2({r_0}^2 + r^2 - 3{r_1}^2)}{({r_0}^2 - {r_1}^2)^3} & \forall\ r_1 < r \le r_0 \\ 0 & \forall\ r > r_0 \end{cases} \quad (9)$$

The long-range interactions were taken into account by the reaction field method.[14,15] Further details about the QMCF methodology are given in ref 16.

2.1. Simulation Details. An important step of a QMCF-MD simulation is the choice of an adequate basis set. A compromise must be found between the computational effort and the accuracy of the results. To reduce the computational effort, a basis set with an effective core potential (ECP) for the chromium atom was chosen. The best basis set was found based on geometry optimizations of $[CrO_4(H_2O)_n]^{2-}$ clusters and chromate water potential scans, namely, the basis set crenbl with ECP for the inner 10 electrons.[17] The double-ζ basis set Dunning dzp[18,19] was employed for hydrogen and oxygen. For the chromate oxygen atoms, the addition of diffuse functions was tested[18,20] by calculations for the gas-phase geometry of the anion and anion water clusters. For larger $[CrO_4(H_2O)_n]^{2-}$ clusters ($n > 5$), $O_{\text{chromate}}-H_{\text{water}}$ distance differences below 4% were observed. For the QMCF simulation, the diffuse functions could be omitted, therefore, because they would lead to an unnecessary computational effort without improving the results. All calculations in the QM regions were performed at the Hartree−Fock level because the use of post-Hartree−Fock methods would imply unaffordable computational time. For the simulation, the canonical NVT ensemble was used. The cubic simulation box (a = 31.1 Å) contained 1000 water molecules and one chromate anion. The MM region was treated by molecular mechanics using the flexible BJH−CF2 model[21,22] for the solvent. The QM region was divided into a core with r = 5.25 Å and the following layer up to r = 7.8 Å. The average number of water molecules in the quantum mechanically calculated region was 52. The temperature of the solution was kept constant at 298.15 K by the Berendsen algorithm.[23] The time step of the predictor−corrector integrator[24] was set to 0.2 fs to explicitly describe the hydrogen movements. The charges on the atoms in the QM regions are represented by their Mullikan point charges.[25] As the starting configuration, an equilibrated box from a tetrahedral anion of a previous simulation[27] was taken. After the insertion of chromate, the box was heated twice (700 and 400 K). After the second heating and cooling down, the simulation was run for 2.0 ps at room temperature for equilibration. Further simulation details are given in the method reference.[16] The overall computation time for the final sampling of 11.4 ps amounted to 9 months on a cluster with eight Opteron dual-core 2.8 GHz processors.

3. Results and Discussion

3.1. Structure. The intramolecular Cr−O distance oscillated between 1.50 and 1.71 Å. During the simulation, the average bond distance was 1.61 Å. Experimental extended X-ray absorption fine structure (EXAFS) spectroscopy data show a Cr−O distance of 1.66 Å.[7] The small difference of 3% could be the result of the neglected electron correlation. The intramolecular O−Cr−O angles oscillate around the ideal tetrahedral angle and result as 109.5° ± 2.0°. The $Cr-O_{\text{water}}$ and $Cr-H_{\text{water}}$ radial distribution functions (RDFs) show a well-defined first shell (Figure 1). The main $Cr-O_{\text{water}}$ distance is between 3.7 and 3.9 Å, and integration of this peak

(12) Frick, R. J.; Pribil, A. B.; Hofer, T. S.; Randolf, B. R.; Bhattacharjee, A; Rode, B. M. *Inorg. Chem.* **2009**, *48*(9), 3993.
(13) Vchirawongkwin, V.; Pribil, A. B.; Rode, B. M. *J. Comput. Chem.* **2010**, *31*(2), 249–257.
(14) Onsager, L. *J. Am. Chem.* **1936**, *58*(8), 1486–1493.
(15) Allen, M. P.; Tildesley, D. J. *Computer Simulation of Liquids*; Oxford Science Publications: Oxford, U.K., 1990.
(16) Rode, B. M.; Hofer, T. S.; Randolf, B. M.; Schwenk, C. F.; Xenides, D.; Vchiawongkwin, V. *Theor. Chem. Acc.* **2006**, *115*, 77–85.
(17) Hurley, M. M.; et al. *J. Chem. Phys.* **1986**, *84*, 6840.
(18) Dunning, T. H. *J. Chem. Phys.* **1970**, *53*, 6026.
(19) Magnusson, E.; SchAfer, H. *J. Chem. Phys.* **1985**, *83*, 5721.
(20) Dunning, T. H.; Hay, P. J. In *Methods of Electronic Structure Theory*, Schaefer, H. F., III, Ed.; Plenum Press: New York, 1977; Vol. 3.
(21) Stillinger, F. H.; Rahman, A. *J. Chem. Phys.* **1978**, *68*(2), 666–672.
(22) Bopp, P.; Janscö, G.; Heinzinger, K. *Chem. Phys. Lett.* **1983**, *98*(2), 129–133.
(23) Berendsen, H. J. C.; Postma, J. P.M.; van Gunsteren, W. F.; DiNole, A.; Haak, J. R. *J. Chem. Phys.* **1984**, *81*, 3648.
(24) Rode, B. M.; Hofer, T. S.; Kugler, M. D. *The Basics of Theoretical and Computational Chemistry*; Wiley-VCH: Weinheim, Germany, 2007.
(25) Mulliken, R. S. *J. Chem. Phys.* **1955**, *97*, 1833.
(26) Pribil, A. B.; Hofer, T. S.; Randolf, B. M.; Rode, B. M. *Chem. Phys.* **2008**, *346*, 182–185.
(27) Pribil, A. B.; Hofer, T. S.; Randolf, B. M.; Rode, B. M. *J. Comput. Chem.* **2008**, *29*(14), 2330–2334.

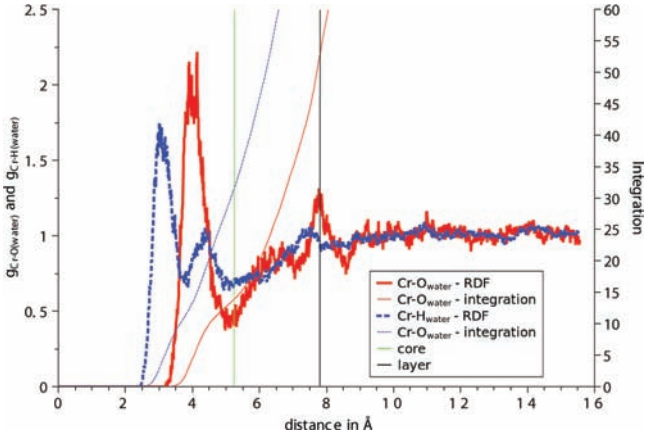

Figure 1. Cr−O_{water} and the Cr−H_{water} RDFs and integration. The limits for core and layer region are indicated.

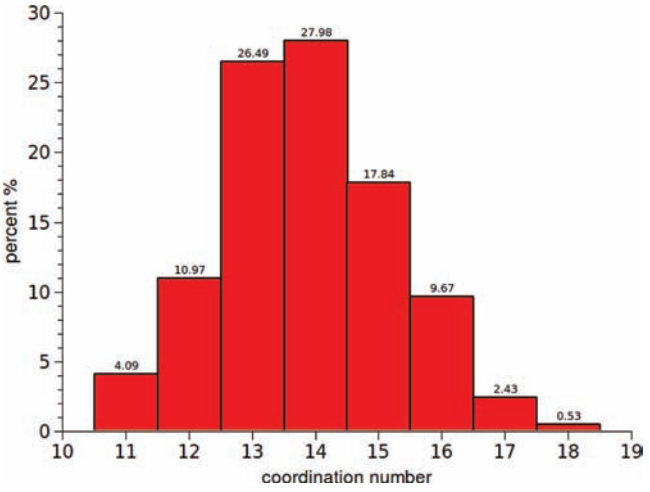

Figure 2. CND of the first hydration shell. The center is the chromium atom, and the upper limit for the Cr−O_{water} distance is 5.25 Å, following the minimum in the RDF.

yields 14 water molecules. A more accurate way to determine the coordination number is the coordination number distribution (CND), which shows a preference for 13 and 14 water molecules in the first hydration shell (Figure 2). The limiting Cr−O distance for this calculation was set to 5.2 Å and corresponds to the minimum in the Cr−O_{water} RDF. Four types of chromate−water binding were found in the hydration shell (Figure 3), with the main type (Figure 3a) representing 90% of all configurations. In this structure type, the water molecules orient themselves with one of their hydrogen atoms to the chromate oxygen atom and the second one to bulk. The remaining 10% are structures with double coordination, as shown in Figure 3b−d. The percentages of these structures are 6.4, 2.1, and 1.6%.

Figure 4 shows the average of the four $O_{chromate}$−H_{water} RDFs, with two distinct maxima. The results of this evaluation are listed in Table 1 and are compared to phosphate,[26,27] sulfate,[26] and perchlorate[26] in water.

Every chromate−oxygen is, on average, coordinated to 2.6 water molecules at a mean $O_{chromate}$−H_{water} distance of 1.82 Å. The comparison of the different tetrahedral anions demonstrates that the chromate is a moderate structure former, similar to sulfate, reflected in the RDFs of these four anions (Figure 5).

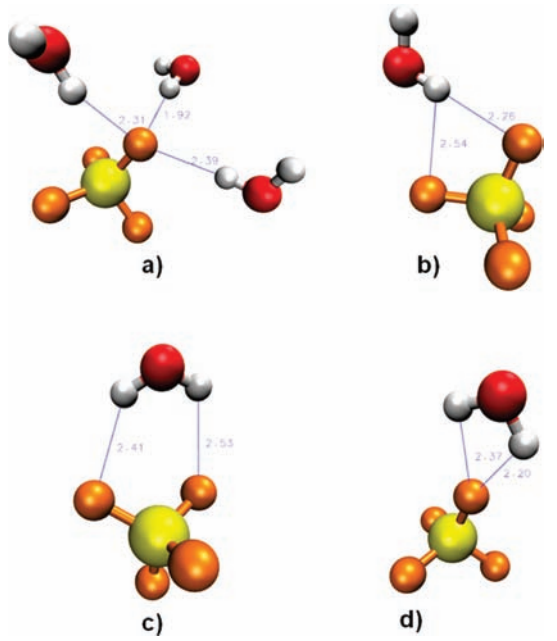

Figure 3. Different chromate−water binding types: (a) the main configuration with singly coordinated water molecules; (b−d) configurations with doubly coordinated water molecules.

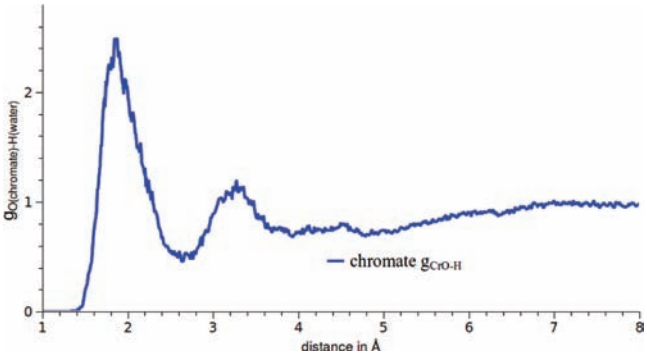

Figure 4. Average of the four $O_{chromate}$−H_{water} RDFs.

Table 1. Comparison of O_{anion}−H_{water} RDFs of the Four Tetrahedral Anions CrO_4^{2-}, ClO_4^-, PO_4^{3-}, and SO_4^{2-}

	CrO_4^{2-}	PO_4^{3-}	SO_4^{2-}	ClO_4^-
reference	this work	26, 27	26	26
r_{max} (Å)	1.82	1.78	1.9	2.1
r_{min}(Å)	2.6	2.5	2.6	2.7
g_{O-H}(max)	2.50	3.75	2.10	1.00

The angular distribution function (ADF) for the Cr−$O_{chromate}$−H_{water} angle is presented in Figure 6. Taking the halfwidth of the ADF into account, the main angles were identified to lie between approximately 100° and 145° within a distributation from 70° to 180°. A linear Cr−$O_{chromate}$−H_{water} bond is only observed for $O_{chromate}$−H_{water} distances above 2.25 Å. The combined treatment of the Cr−$O_{chromate}$−H_{water} angle and the $O_{chromate}$−H_{water}−O_{water} angle shows that the $O_{chromate}$−H_{water}−O_{water} angle assumes values above 150° for water molecules in the hydration sphere. The rare Cr−$O_{chromate}$−H_{water} angles near 180° represent an approximately linear Cr−$O_{chromate}$−H_{water}−O_{water} bond. The structural properties are summarized in Table 2.

3.2. Dynamic Properties. Important data for the dynamical properties of solutions result from IR and/or Raman

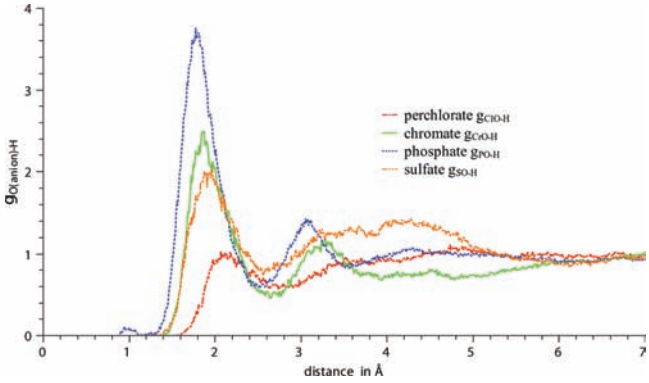

Figure 5. Comparison of the $O_{anion}-H_{water}$ RDFs of PO_4^{3-}, SO_4^{2-}, CrO_4^{2-}, and ClO_4^- showing the different stabilities of the hydration shell.

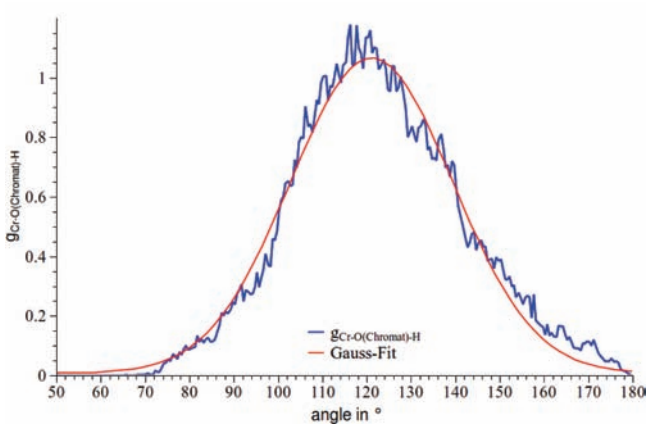

Figure 6. ADF of the $Cr-O_{chromate}-H_{water}$ angle.

Table 2. Structural Properties of the Chromate Anion and Its Hydration Shell

	CrO_4^{2-}	comment
$Cr-O_{chromate}$(average) (Å)	1.61	
$O_{chromate}-H_{water}$(average) (Å)	1.82	
O−Cr−O angle (intramolecular) (deg)	109.5 ± 2.0	for 2σ
$Cr-O_{chromate}-H_{water}$ angle (deg)	117	maximum
main coordination numbers (center = Cr; r = 5.25 Å)	13 and 14	
coordination number (center = $O_{chromate}$; r = 2.6 Å)	2.5	

spectroscopy. From the irreducible representations, the normal modes of a given geometry can be calculated. A method to obtain a vibrational spectrum from a QMCF-MD simulation is the Fourier-transformed velocity autocorrelation function (VACF),[26] and this evaluation of the chromate simulation is shown in Table 3. The comparison with experimental data demonstrates the high accuracy of the QMCF-MD methodology.

The minima of the RDFs (Figures 1 and 4) do not reach zero, which is an indication of ligand exchange between the hydration shell and bulk. The fact that the RDF is nonzero between hydration shells is not necessarily an indication of ligand exchanges but may simply be a result of overlapping broad peaks. Because the respective intensities are considerably large (roughly 0.5 for the $Cr-O_{water}$ and $O_{chromate}-O_{water}$ pair distribution), exchange events may

(28) Xenides, D.; Randolf, B. M.; Rode, B. M. *J. Chem. Phys.* **2005**, *122* (17), 174506.

Table 3. Wavenumbers (cm^{-1}) of the Normal Modes from the Simulation

mode	simulation[a]	Michel[b,31]	Stammreich[c,32]	Ramsey[d,33]
$\nu_1(A_1)$	356	348	348	348
$\nu_2(E)$	396	371	368	370
$\nu_3(T_2)$	854	846	847	848
$\nu_4(T_2)$	881	887	884	865

[a] Intramolecular vibration modes are scaled by 0.89, according to refs 29 and 30. [b] 0.1 M K_2CrO_4, pH = 11. [c] No details reported. [d] Dilute solution, pH = 8−10.

Table 4. Dynamic Properties of Hydrated Chromate, Perchlorate, Phosphate, Sulfate, and of Pure Water: MRTs (τ Values in ps), Coordination Number CN, Number of Accounted Exchange Events N, and Average Number of Attempts Needed To Achieve a Lasting Exhange Event R_{ex}

anion	$\tau_{0.5}$	τ_0	CN	$N_{ex}^{0.5}$	N_{ex}^{0}	R_{ex}	ref
Sphere Surrounding the Whole Anion							
chromate	2.3	0.6	14	70	273	3.9	this work
perchlorate	1.5		10				26
phosphate	3.9	0.9	13	42	132	3.1	26, 27
sulfate	2.6	0.3	11	54	399	7.4	26
water	1.7	0.2		24	269	11.2	28
Sphere Surrounding the Anion Oxygen Atoms							
chromate	1.1	0.9	2.6	28	343	12.3	this work
Cr−O Distance of 2.6 Å; $Cr-O_{chromate}-H_{water}$ Angle of 100−145°							
chromate	0.8	0.1	2.0	28	337	12.0	this work

be expected. These exchange processes can be analyzed by mean ligand residence times (MRTs). MRTs were calculated by direct methods[34] and amount to 2.2 ps for the overall solvation shell around the chromate anion ($r_{Cr-O} \leq$ 5.25 Å) and 1.0 ps for the separate hydration shells surrounding the chromate oxygen atoms ($r_{O\ldots H} \leq 2.6$ Å). All of these values were calculated for exchange processes lasting more than 0.5 ps, which had been found to be the most appropriate value.[34] Table 4 compares the values for $t^* = 0.5$ and 0 ps. These two values allow one to determine how many attempts are needed to achieve one successful exchange between the hydration shell and bulk water. In addition, Table 4 contains the results for phosphate, sulfate, and pure water. The immediate vicinity of the chromate can be defined in different ways, either considering spherical regions centered on each of its oxygen atoms or taking into account a large sphere centered on the chromium atom. The MRT values obtained from the two definitions are significantly different, which results mainly from the excluded and overlapping volumes occurring when oxygen-centered volumes are employed to define the first hydration layer. The main discrepancy results from intershell migration, which is not considered when the entire first shell is taken into account and, consequently, the MRT in that case is larger and classifies chromate as a weak structure-forming anion.

3.3. Hydrogen Bonding. It is important to characterize hydrogen bonds between the solute and solvent because they

(29) Scott, A.; Radom, L. *J. Phys. Chem.* **1996**, *100*, 16502.
(30) Defrees, D.; McLean, A. *J. Chem. Phys.* **1985**, *82*(1), 333.
(31) Michel, G.; Machiroux, R. *J. Raman Spectrosc.* **1983**, *14*(1), 22–27.
(32) Stammreich, H.; Bassi, D.; Sala, O. *Spectrochim. Acta* **1958**, *12*, 403.
(33) Ramsey, J. D; Xia, L.; Kendig, M. W.; McCreery, R. L. *Corros. Sci.* **2001**, *43*(8), 1557–1572.
(34) Hofer, T. S.; Tran, H. T.; Schwenk, C. F.; Rode, B. M. *J. Comput. Chem.* **2004**, *25*, 211–221.

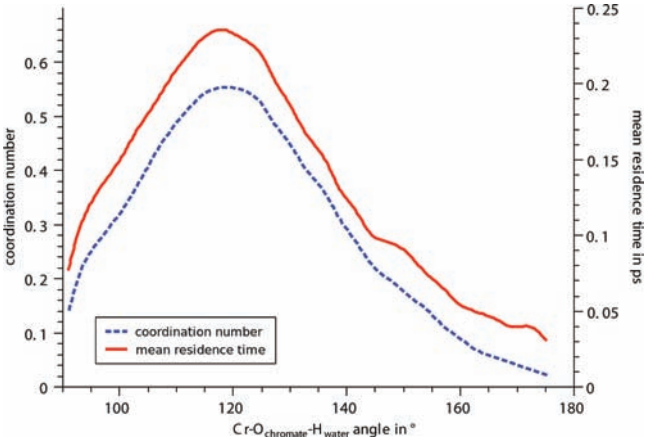

Figure 7. Coordination numbers and MRTs of different spherical sectors. Every point x of the functions corresponds to a sector, which includes Cr−O$_{chromate}$−H$_{water}$ angles between $(x - 5)°$ and $(x + 5)°$.

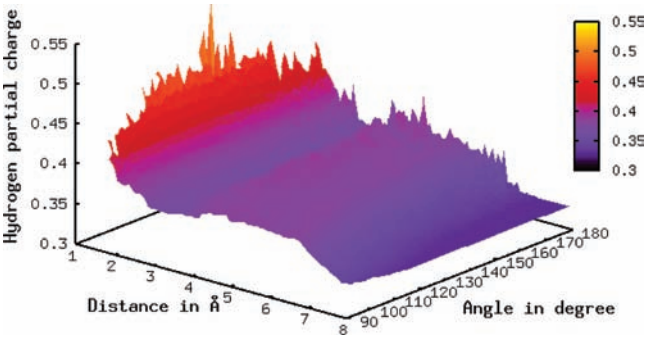

Figure 8. Mulliken point charges as a function of the O$_{chromate}$−H$_{water}$ distances and Cr−O$_{chromate}$−H$_{water}$ angles. Higher point charges indicate a stabilizing interaction.

stabilize the hydrate complex. Therefore, the MRTs and CNDs for different spherical sectors, representing the different Cr−O$_{chromate}$−H$_{water}$ angles, were calculated, and the results are shown in Figure 7. The most stable region is within Cr−O$_{chromate}$−H$_{water}$ angles of 100−145°. In combination with the O$_{chromate}$−H$_{water}$ RDF (Figure 4), a stabilizing region for hydrogen bonds can be identified. Another approach to this region is the analysis of the Mulliken charges. If H$_{water}$ and O$_{chromate}$ interact, the point charge on the hydrogen must rise. Figure 8 shows the result of this evaluation. The range for interaction is nearly identical with the combined evaluation of the MRT and RDF. Inside this region of interest (r = 0−2.6 Å; θ = 100−145°), the structural and dynamic properties were calculated and listed in Table 4. The coordination number in this region is 2.0, and, consequently, more than 75% of the water molecules inside the hydration shell are in this region. The MRT (t^* = 0.5 ps) amounts to 0.8 ps. Iijima reported ν_{OH} of the hydrogen bond between 170 and 210 cm^{-1}.[35] A VACF analysis of our simulation generated a spectrum with an absorption maximum at 185 cm^{-1}.

4. Conclusion

Detailed information about the hydration structure and dynamics of chromate in aqueous solutions could be obtained, and the results correspond well with experimental EXAFS and Raman data. The first hydration shell of the chromate anion consists of 14 water molecules. Each chromate oxygen is, on average, bound to 2.6 water molecules at a mean distance of 1.82 Å. The MRT of the first shell water molecules was evaluated as 2.2 ps by employing a direct counting of exchange events. The chromate anion is a moderate structure building ion, similar to the sulfate anion. The comparison with other tetrahedral anions results in the following order of structure-forming properties: ClO_4^- < SO_4^{2-} < CrO_4^{2-} < PO_4^{3-}.

Different evaluations lead to a region (r = 0−2.6 Å; θ = 100−145°) in the vicinity of the chromate oxygen atoms, in which hydrogen bonds are preferentially formed.

Acknowledgment. Financial support for this work by the Austrian Science Foundation is gratefully acknowledged.

Supporting Information Available: Average binding energies for CrO_4^{2-}−H_2O clusters. This material is available free of charge via the Internet at http://pubs.acs.org.

(35) Iijima, T. *J. Mol. Struct.* **1996**, *376*(5), 525–529.